Computational Biology and Chemistry 35 (2011) 371–380

Contents lists available at SciVerse ScienceDirect

Computational Biology and Chemistry

journal homepage: www.elsevier.com/locate/compbiolchem

Research Article

# Detecting breakdown points in metabolic networks

Somnath Tagore [a], Rajat K. De [b,*]

[a] Department of Biotechnology and Bioinformatics, Dr DY Patil University, Navi Mumbai 400614, India
[b] Machine Intelligence Unit, Indian Statistical Institute, Kolkata 700108, India

ARTICLE INFO

*Article history:*
Received 27 September 2011
Accepted 1 October 2011

*Keywords:*
Graph theory
Breakdown
Perturbation
Resilience
Robustness

ABSTRACT

*Background:* A complex network of biochemical reactions present in an organism generates various biological moieties necessary for its survival. It is seen that biological systems are robust to genetic and environmental changes at all levels of organization. Functions of various organisms are sustained against mutational changes by using alternative pathways. It is also seen that if any one of the paths for production of the same metabolite is hampered, an alternate path tries to overcome this defect and helps in combating the damage.
*Methodology:* Certain physical, chemical or genetic change in any of the precursor substrate of a biochemical reaction may damage the production of the ultimate product. We employ a quantitative approach for simulating this phenomena of causing a physical change in the biochemical reactions by performing external perturbations to 12 metabolic pathways under carbohydrate metabolism in *Saccharomyces cerevisae* as well as 14 metabolic pathways under carbohydrate metabolism in *Homo sapiens*. Here, we investigate the relationship between structure and degree of compatibility of metabolites against external perturbations, i.e., *robustness*. Robustness can also be further used to identify the extent to which a metabolic pathway can resist a mutation event. Biological networks with a certain connectivity distribution may be very resilient to a particular attack but not to another. The goal of this work is to determine the exact boundary of network breakdown due to both random and targeted attack, thereby analyzing its robustness. We also find that compared to various non-standard models, metabolic networks are exceptionally robust. Here, we report the use of a 'Resilience-based' score for enumerating the concept of 'network-breakdown'. We also use this approach for analyzing metabolite essentiality providing insight into cellular robustness that can be further used for future drug development.
*Results:* We have investigated the behavior of metabolic pathways under carbohydrate metabolism in *S. cerevisae* and *H. sapiens* against random and targeted attack. Both random as well as targeted resilience were calculated by formulating a measure, that we termed as 'Resilience score'. Datasets of metabolites were collected for 12 metabolic pathways belonging to carbohydrate metabolism in *S. cerevisae* and 14 metabolic pathways belonging to carbohydrate metabolism in *H. sapiens* from Kyoto Encyclopedia for Genes and Genomes (KEGG).


## 1. Introduction

Various biological processes in living organisms are defined by their internal functional or physical reactions with different genes or proteins. There are various on-going characterizations of interactions, viz., metabolic, signal transduction and gene regulatory pathways (Kreeger and Lauffenburger, 2010). Biological pathways are analyzed and modeled for visualizing networks, sub-steps of pathways, measuring gene expression levels, predicting outcome of various alterations made to the cells and identifying intracellular targets for drugs and genetic engineering (Acencio and Lemke, 2009). While modeling approaches have a long history in biochemical reactions and enzyme kinetics, the importance of modeling complex reactions, biochemical pathways and networks has only recently begun to be appreciated by the wider community of biochemical researchers (Schmidt and Jacobsen, 2004).

Several approaches for modeling pathways include symbolic modeling, quantitative modeling, adaptive modeling, analytical modeling, discrete modeling and machine learning. Symbolic modeling is an approach for modeling cellular processes based on some known constraints (Bongard and Lipson, 2007). Quantitative modeling of biochemical networks can be done using 'graphs' and 'network theories' (Kitano, 2001). In adaptive modeling, global or local pathways are modeled by many differential equations (Jeong et al., 2000). Analytical models involve formulation of some differential equations representing dynamics of the system parameters

* Corresponding author. Tel.: +91 9433008009; fax: +91 3325783357.
*E-mail address:* rajat@isical.ac.in (R.K. De).

1476-9271/$ – see front matter © 2011 Elsevier Ltd. All rights reserved.
doi:10.1016/j.compbiolchem.2011.10.007

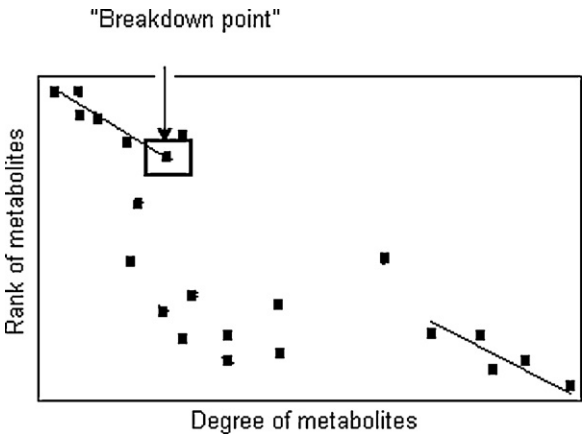


**Fig. 1.** Plotting breakdown point mathematically.

(algebraic, integral-differential, finite-differential, etc.) based on logical conditions (Palsson, 2006). Dynamic models are generally based on flux calculations (Palsson, 2006). Discrete models are based on state transition diagrams (Glass and Siegelmann, 2000). In this study, we use the quantitative approach consisting of graphs and network theories for analyzing metabolic networks.

Recent advances in screening technologies have made it possible to construct large-scale visualizations of protein interaction networks, metabolic networks and gene regulatory networks for a number of organisms. Motivated by these developments, there has been a significant amount of work on identifying and interpreting the structural properties of these networks, such as degree distributions, characteristic path lengths, modular structure, robustness measures and local clustering properties (Barabasi et al., 2000).

Our focus in this work is analyzing 'breakdown points' in metabolic networks. We define 'breakdown points' as those instances where removing or modifying certain metabolites drastically effects the overall functioning of a metabolic pathway. For example, in a metabolic network, removal of an enzyme or a metabolite and its corresponding reaction causes the malfunction and knockout of various additional reactions (Arita, 2005; Barabasi and Albert, 2002). A network breakdown can be analyzed by plotting a 'power-law curve' for the metabolite dataset. A power-law is a relationship between two entities, e.g., frequency of a metabolite (entity 1) and total occurrence of that metabolite (entity 2) in a given dataset (Destexhe and Touboul, 2010). The entities are inversely proportional on log-log scale. Normally, most of the datasets follow the power law (Mitzenmacher, 2003). The 'breakdown point' is the threshold after which the main component of the metabolic network starts disintegrating. It can be defined as the point at which the log-log data cannot be fitted linearly using the error of fitting as the criteria. For instance, Fig. 1 shows the exact breakdown point in a hypothetical metabolic pathway where the line could not be fitted properly.

Thus, network breakdown occurs when there is a sudden change in the plot due to some external or internal perturbation. For this reason, a balance needs to be maintained against perturbations while being adaptable in the presence of changes, a property known as *robustness* (Callaway et al., 2000). Studies on the topological and functional properties of metabolic networks have achieved some progress, but still have limited understanding of robustness of metabolic pathways. Furthermore, more important a reaction is, higher is the chance to have a backup reaction. Thus, removing an enzyme or a metabolite from a reaction may lead to blocking the production of the successive product, but an alternate reaction may ultimately produce this necessary metabolite (Bulik et al., 2009).

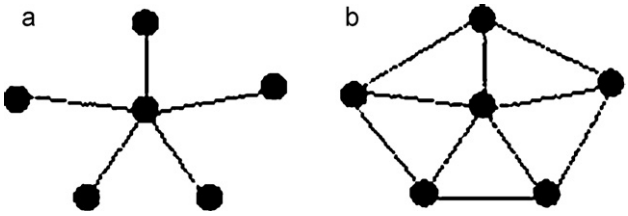


**Fig. 2.** Network showing probability of fragmentation.

The robustness of a model can also be assessed by means of altering the various parameters and components associated with forming a particular metabolite. For instance, certain co-factors and associated molecules can be removed to check their role in metabolite formation. It is presumed that a model in which the parameter sensitivities are relatively low will be more robust (Westerhoff et al., 2009; Wit and Khanin, 2006). We have studied robustness of a network with respect to 'resilience', which is defined as a method of analyzing the sensitivities of internal constituents under external perturbation, that may be random or targeted in nature (Barabasi and Albert, 2002).

Furthermore, networks with a given degree distribution may be very resilient to one type of attack but not to another. Consider the six node network in Fig. 2a. It is relatively robust with respect to a random failure – only a failure of the central node will cause the network to fragment; the probability for fragmentation of the network being 1/6. Similarly, it is extremely vulnerable to a targeted attack; the probability for fragmentation of network being 1. As shown in Fig. 2b, we can modify the network to make it more resilient and increase its robustness to targeted attack, where neither a single node under random failure nor a targeted attack to remove only one node can fragment the network (Cohen et al., 2000; Macia and Sol, 2009). Now, we define a property known as 'fitness' associated with all metabolites, as their degree of resistance against knockouts, i.e., the means by which they counteract with their removal. For instance, this resistance can be in terms of its continuous production using some other backup reactions present in the metabolic pathway.

We can also study biological networks as random in nature having scale-free and bimodal degree distribution. Scale-free networks exhibit degree distributions of the form $p(lk) \propto lk^{\lambda}$, for characterizing resilience, where $lk$ denotes links between lth and $k$th metabolite pairs, $p$ is probability of occurrence of links and $\lambda$ is a constant (Takemoto and Oosawa, 2007). For large scale-free networks with exponent $\lambda < 3$, it has been found that if nodes fail randomly, essentially all nodes must fail for the network to become disconnected (Minnhagen and Bernhardsson, 2008).

In this work, we have performed both random as well as targeted external perturbations for identifying the breakdown points in metabolic pathways and checking their 'robustness' to external attacks (Macia and Sol, 2009; Mendes et al., 2009). Studying the robustness of a metabolic network helps in identifying the changes in the metabolic makeup of an organism occurred during modifications or perturbations, caused by deletions of genes coding for enzymes, which results in a loss of the corresponding biochemical conversions. Furthermore, resilience has also been used to study the robustness of metabolic pathways against both random and targeted attack. The 'resilience score' calculated by us successfully gives an insight into the exact number of metabolites that can be removed for damaging the overall functioning of the metabolic network. The pathway datasets chosen for testing were collected from Kyoto Encyclopedia for Genes and Genomes (KEGG) (Kawashima et al., 2004). The work was done on 12 and 14 metabolic pathways under carbohydrate metabolism in *Saccharomyces cerevisae* and *Homo sapiens* respectively.

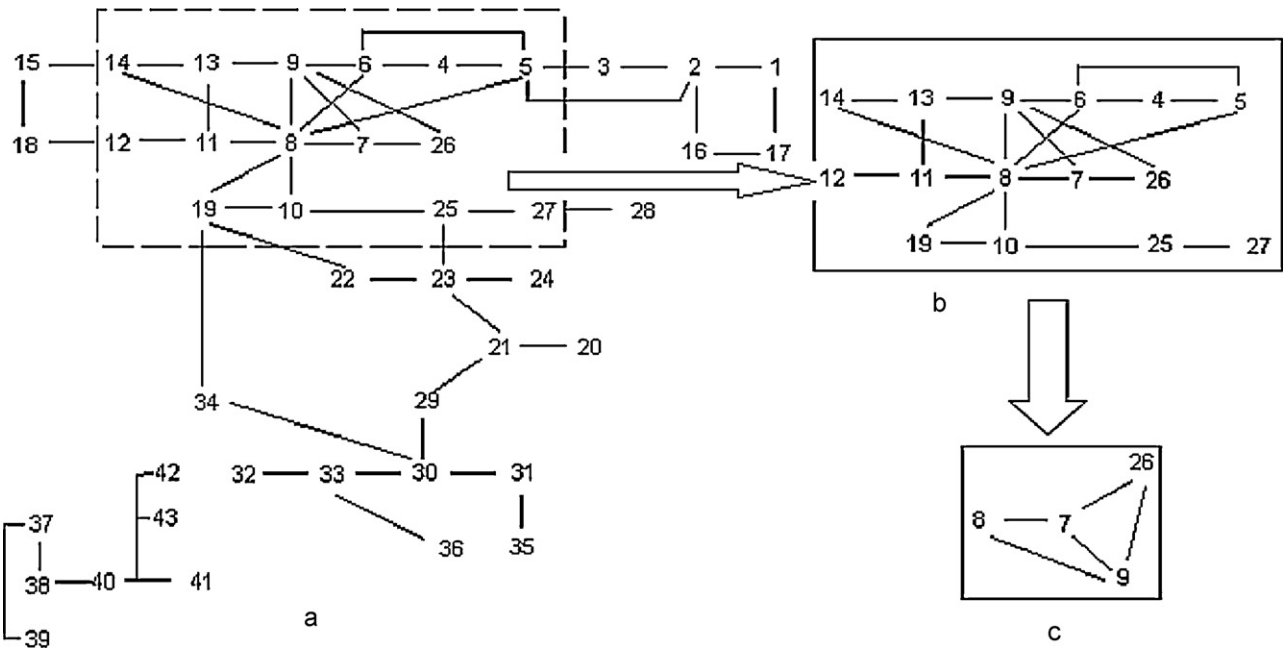


**Fig. 3.** (a) Graphical representation of aminosugars metabolism in *H. sapiens*, (b) giant component, (c) node '7' is the core metabolite of the giant component. The metabolites are 1: CMP-N-acetyl neuraminate, 2: N-acetyl neuraminate, 3: N-acetyl neuraminate-9P, 4: N-acetyl D-mannosamine, 5: N-acetyl D-mannosamine-6P, 6: UDP-N-acetyl D-glucosamine, 7: N-acetyl-α-D-glucosamine-6P, 8: D-glucosamine-6P, 9: N-acetyl D-glucosamine-6P, 10: D-fructose-6P, 11: D-glucosamine, 12: D-glucosaminide, 13: N-acetyl D-glucosamine, 14: chitobiose, 15: chitin, 16: N-glycoloyl neuraminate, 17: CMP-N-glycoloyl neuraminate, 18: chitosan, 19: fructose, 20: UDP-Rha, 21: UDP-4-keto Rha, 22: D-Glc-1P, 23: UDP-D-Api, 24: UDP-L-IdoA, 25: UDP-D-Xyl, 26: D-Xyl-1P, 27: 1,4-β-D-xylan, 28: D-Xyl, 29: UDP-SQ, 30: UDP-GalA, 31: pectin, 32: GalA, 33: GalA-P, 34: α-Gal, 35: GDP-L-Gul, 36: GDP-L-Gal, 37: GDP-Glc, 38: CDP-Glc, 39: ADP-Glc, 40: CDP-4 keto-6-deoxy-D-Glc, 41: CDP-paratose, 42: CDP abequose and 43: CDP ascarylose.

## 2. Methodology

Here we describe the method we have developed for detecting breakdown points in metabolic networks corresponding to carbohydrate metabolism in *S. cerevisae* and *H. sapiens* as well as under external perturbation. According to network theory, the extent of tolerance of metabolic pathways against an external perturbation signifies the level of robustness (Kitano, 2007). Whenever we talk about robustness of a metabolic pathway, we need to emphasize on some key issues due to which a standard pathway needs to face extraordinary situations. For instance, these situations include changes in external environment of the organism, evolutionary changes in the cell, mutational events and so on (Adami and Hintze, 2008). Furthermore, due to these changes, a standard metabolic pathway needs to adjust itself for proper functioning and overall development of the organism. Moreover, each metabolic pathway differs in its method of adjustment and the manner in which they handle these stressful situations (Doyle and Stelling, 2009). For example, a lipid metabolic pathway will adjust itself in a different manner than an amino acid pathway for the same external environment change. In this study, we try to focus on the key metabolites, whose removal may drastically reduce the extent of robustness and overall functioning of the pathway. We term these key metabolites as 'breakdown metabolites' and the steps at which these metabolites are removed from the pathway as 'breakdown points'.

The strategy that we have chosen for such analysis is based on graphs. Graph-based analysis or quantitative analysis is used to represent the metabolic pathways mathematically in terms of metabolites and their reaction links (Bullmore and Sporns, 2009). Here the method of network breakdown analysis uses graph-based strategies for identifying these key points. Let us consider the aminosugars metabolism in *H. sapiens* consisting of 43 metabolites and 58 reaction links (Fig. 3). We represent the given pathway as a graph $G(V, E)$, where $V$ is the set of 'vertices' or 'nodes' indicating metabolites and $E$ is the set of 'edges' depicting 'reaction links'.

The graph-based representation of aminosugars metabolism in *H. sapiens* is shown in Fig. 3a. Before proceeding with the description of the algorithm, we define some terms like 'degree', 'clustering coefficient', 'average clustering coefficient', 'giant component', 'rank' and 'resilience' (Bullmore and Sporns, 2009; Deo, 2003).

In an undirected graph, 'degree' $d_i$ of $i$th node is defined as the number of links attached to it (Deo, 2003). Thus in Fig. 3a, $d_7 = 3$, $d_8 = 8$ and so on. The term 'clustering coefficient' $c_i$ of $i$th node is defined as $c_i = 2 \times D_i/[d_i \times (d_i - 1)]$, for $d_i \geq 2$; where $D_i$ is the number of links among the neighboring nodes of $i$th node (Stumpf and de Silva, 2005). For $d_i \leq 2$, we define $c_i = 0$. Thus, $c_7 = 0.6$, $c_8 = 0.2$, $c_{10} = 0.3$, $c_{25} = 0$ and so on (Fig. 3a). 'Average clustering coefficient' $c_G = \sum c_i/N$, where $N$ is the number of metabolites in the pathway (Stumpf and de Silva, 2005). Thus, $c_G = 0.069$ (Fig. 3a). A 'giant component' $G_c$ is defined as the largest fully connected part of a metabolic network (Fig. 3b). Also, the core metabolite of $G_c$ tends to have the highest $c_i$ value, over the nodes in $G_c$ and is termed as $g_c$. Thus, in Fig. 3c, $g_c = 7$ (Zeng and Ma, 2003). The term 'rank' $r_i$ of $i$th node is defined as its position in the list of degrees of nodes, where the list is made on sorted descending order of degrees. Thus, in Fig. 3, $r_7 = 6$, $r_8 = 1$ and so on. Finally, 'resilience' $\gamma$ is defined as the ratio of number of nodes removed after which breakdown occurs, to the total number of nodes in the pathway (Sudakov and Vu, 2008). In the given schematic diagram of aminosugars metabolism in *H. sapiens* (Fig. 3a), node 8 (D-glucosamine-6P) has the highest number of links (i.e., 8), and is associated with 8 nodes by direct links. These nodes represent, N-acetyl D-glucosamine-6P (9), UDP-N-acetyl D-glucosamine (6), N-acetyl-α-D-glucosamine-6P (7), D-fructose-6P (10), fructose (19), D-glucosamine (11), N-acetyl D-glucosamine (13) and, N-acetyl-D-mannosamine-6P (5), and acts as a 'hub'. The characteristics of hubs are that they are extremely important for the overall functioning of the metabolic pathway as they are involved in large number of reactions. Knock-out of any of the hubs from a metabolic network is lethal to its functioning,

as it may knock-out several other interconnected and successive metabolites. A property associated with 'hub-ness' is 'centrality' that deals with characterizing the hubs in the metabolic networks, whereas another property, called 'essentiality' deals with identifying all those metabolites whose removal is lethal to the overall functioning of the metabolic pathway (Sudakov and Vu, 2008).

We have analyzed the breakdown points of metabolic networks using 'power-law modeling'. For analyzing metabolic pathways using power-laws, we have taken into consideration the 'degree' and 'rank' of metabolites. We plot the 'ranks' vs 'degrees' on a log–log scale and check whether an inverse plot is obtained. We also check for the point where the log–log date cannot be fitted linearly (Mitzenmacher, 2003). These pathways are termed as 'scale-free' or 'hierarchical'. If there is some uneven pattern other than an inverse plot, we say that the metabolites belong to a 'random' network (Mitzenmacher, 2003). The difference between a 'scale-free' and 'hierarchical' network is that in 'hierarchical', the 'average clustering coefficient' $c_G \simeq 0.6$ (Barabasi and Albert, 2002; Arita, 2005; Rikvold, 2007).

For analyzing the extent of tolerance by metabolic pathways against external perturbation, we have taken into consideration a property called 'robustness', i.e., the means by which pathways resist or combat during the course of perturbation (Cohen et al., 2000; Zhang and Zhang, 2009). In this study, we have measured this tolerance using resilience. We have simulated this phenomenon of attack by removing the metabolites already present in the metabolic pathway, i.e., performing a deletion mutation. We have categorized attack as random and targeted based upon the nature of perturbation, i.e., whether the metabolites are removed randomly or in a specific manner by targeted selection (Barabasi et al., 2000). Next, we calculate the degree of the remaining metabolites along with their ranks. This is followed by plotting a power-law of the degrees ($x$-axis) for these remaining metabolites and their ranks ($y$-axis) on a log–log scale (Mitzenmacher, 2003). We repeatedly perform this removal as well as plotting, and identify the position at which a sudden breakdown of power-law occurs. We define this position as the 'breakdown point' and hypothesize that the metabolite selected for removal just before the power-law breaks is an essential metabolite, whose removal causes serious damage to the functioning of the pathway (Zhang and Zhang, 2009).

In case of random attack, we remove metabolites from the pathway in a random manner. The removed metabolites are included in a group $R$. The remaining metabolites are assigned to a group $R^l$. Our proposed approach has two different methods of storing metabolites in $R$. Method 1 (discussed later) removes the metabolites one by one, puts in $R$ and performs further analysis using $R^l$ (i.e., rest of metabolites). Method 2 (also discussed later) removes the metabolites one by one, but adds it back to the network (i.e., in $R^l$), when a different metabolite is selected. Thus, at any instance only one metabolite is present in $R$, whereas in case of Method 1, $R$ may consist of more than one metabolite at any given instance. Now, we plot power-law curve for the metabolites present in $R^l$ and repeat the steps until power-law breaks. Next we calculate a measure called 'random resilience score', $R^s$ = ratio of number of metabolites removed randomly until power law breaks, to the total number of metabolites (Cohen et al., 2000). Similarly, in targeted attack, specific metabolites are removed from the pathway, followed by constructing a power law curve. One of the essential pre-requisite for targeted removal is selection of the appropriate metabolite for removal. For each metabolite, clustering coefficient $c_i$ is calculated. We say that the metabolite having the highest $c_i$ is the core metabolite $g_c$ of giant component $G_c$ (Zeng and Ma, 2003). We put these metabolites in $T$ according to their $c_i$ values in descending order. The metabolites present in $T$ are now targeted for removal, one after the other, followed by plotting the power-law curve. This is repeated until the power-law breaks. Again we calculate 'targeted resilience score', $T^s$ = ratio of number of targeted metabolites removed until power law breaks to the total number of metabolites. We have implemented the method using the pathway of aminosugars metabolism in *H. sapiens* (Fig. 3a) (in Supplementary information).

## 3. Results

We have demonstrated the effectiveness of the above method on 12 and 14 metabolic pathways under carbohydrate metabolites in *S. cerevisae* and *H. sapiens*, respectively, for exhibition of network breakdown and their corresponding resilience measure (Tables 1 and 2 in Supplementary information). In case of random attack, a pseudo-random unique number array is generated and used to simulate random removal of nodes from the graph. The determination of power law distribution of networks is made by analyzing the log–log power law plot in each case. Where a majority of points appears to be following an inverse line, power law is being followed (Callaway et al., 2000). The points may appear to fall along a curve since they have been plotted on a log–log scale but a rough inverse pattern being followed would mean a power law distribution. As a property of log–log scales, the lines will be straight with a large number of points being plotted. Conversely, in cases where a clear majority of points are not along an inverse line, power law is deemed to fail. Also, in cases where only two points are available to be plotted, power law distribution cannot be determined as two points will always be on a straight line whether or not they are following a power law (Ravasz, 2009). One can notice a sharp change in the distribution of power law depicting the breakdown of the network. Tables 3–6 (in Supplementary information) give insight about the analysis using both the methods. We have used certain notations in these tables. These include 'FP' as following power-law, 'NP' as not following power-law and 'NOT' as not found. The notations for the metabolic pathways taken into consideration in this study are aminosugars metabolism ($YN_1$), butanoate metabolism ($YN_2$), fructose mannose metabolism ($YN_3$), galactose metabolism ($YN_4$), glyoxylate metabolism ($YN_5$), glycolysis ($YN_6$), pentose phosphate pathway ($YN_7$), citric acid cycle ($YN_8$), inositol phosphate metabolism ($YN_9$), propanoate metabolism ($YN_{10}$), pyruvate metabolism ($YN_{11}$), starch and sucrose metabolism ($YN_{12}$) in *S. cerevisae* whereas ascorbate and aldarate metabolism ($HN_1$), aminosugars metabolism ($HN_2$), butanoate metabolism ($HN_3$), fructose mannose metabolism ($HN_4$), galactose metabolism ($HN_5$), glycolysis ($HN_6$), pentose phosphate pathway ($HN_7$), citric acid cycle ($HN_8$), inositol phosphate metabolism ($HN_9$), glyoxylate and dicarboxylate metabolism ($HN_{10}$), pentose glucuronate interconversions ($HN_{11}$), propanoate metabolism ($HN_{12}$) and pyruvate metabolism ($HN_{13}$) in *H. sapiens* respectively.

### 3.1. Locating breakdown points in local metabolic pathways under carbohydrate metabolism in S. cerevisae

A breakdown point is defined as the stage beyond which fragmentation of the pathway occurs under external perturbation. Breakdown can be random and/or targeted. We have identified these points by studying the power-law distribution of the corresponding network. Locating these points also highlight the metabolites that are extremely essential for the overall functioning of the pathway. We have found breakdown points for these pathways. For instance, the highest number of breakdown points has been found out in networks $YN_1$, $YN_3$, $YN_6$, $YN_7$ and $YN_{12}$ (random removal), using Method 1, whereas none of the breakdown points have been found out using targeted attack. In $YN_1$, N-acetylneuraminate (connectivity = 9) and N-acetyl-D-glucosamine 6P (connectivity = 10) have almost similar number of connected neighbors, thus contributing almost equally to the functioning of the network. Similarly, breakdown points in the other metabolic

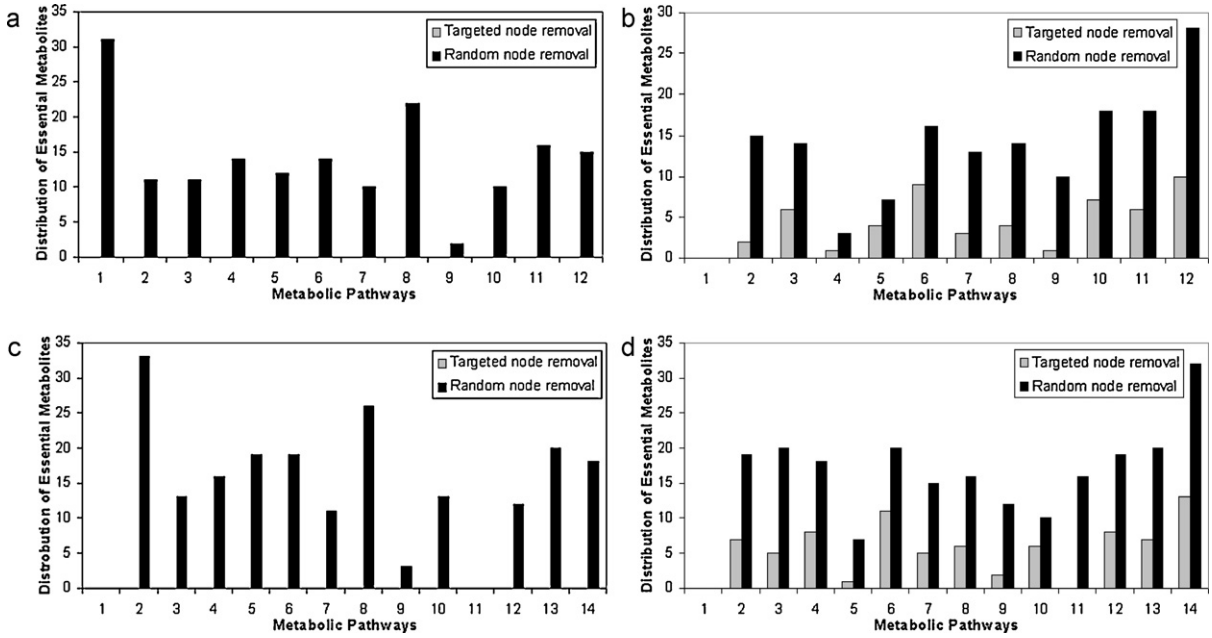


**Fig. 4.** Essential metabolites: (a) *S. cerevisae* Method 1, (b) *S. cerevisae* Method 2, (c) *H. sapiens* Method 1, (d) *H. sapiens* Method 2.

pathways have been found in the same manner (Table 3 in Supplementary information).

Using Method 2 (Table 4 in Supplementary information), breakdown points in both random and targeted attack has been found except for $YN_8$. The network for which the highest number of breakdown metabolites is detected is $YN_1$. They are N-acetyl-D-glucosamine 6P, N-acetyl-D-glucosamine, UDP-glucose, GDP-mannose (random) and D-glucose 1P, UDP-glucuronate, D-glucosamine, D-glucosamine 6P, UDP-D-galacturonate, N-acetyl-D-mannosamine (targeted). Another network for which many breakdown metabolites have been found is $YN_6$, for which the breakdown metabolites are β-D-fructose 6P, phosphoenolpyruvate, acetaldehyde, D-glyceraldehyde-P, 3-phospho-D-glycerate (random) and α-D-glucose, α-D-glucose 6P, β-D-glucose 6P, oxaloacetate, succinate, succinyl-CoA (targeted) (Schmidt et al., 2011). We have also found the 'average clustering coefficient' of all the metabolic pathways under carbohydrate metabolism (Table 5 in Supplementary information). Accordingly, we have observed that all the metabolic pathways under carbohydrate metabolism are scale-free in nature. None of the metabolic pathways are random or hierarchical, and all of them follow power-law distribution (Hacking, 2008). An important feature of this analysis is detection of the 'core metabolite' of 'giant component'. A 'giant component' is defined as a highly connected component of a network having most of the metabolite links. Detecting a giant component increases the chance of detecting the most valuable cluster of metabolites in the network (Cohen et al., 2000). It is also suggested that the giant component is the oldest among all metabolite clusters and that the other metabolites have evolved during the course of evolution (Adami and Hintze, 2008). We define the highest connected metabolite as the 'core metabolite' of 'giant component'. For none of the metabolic pathways studied, core metabolite of giant component is found. We have also calculated the essential metabolites in carbohydrate metabolism for both Methods 1 and 2 (Fig. 4a and b).

### 3.2. Locating breakdown points and characterizing essential metabolites under carbohydrate metabolism in H. sapiens

Continuing our study on *S. cerevisae*, we correlate it with that of *H. sapiens*. This is due to the fact that as long as we deal with metabolism, we can substitute *H. sapiens* with *S. cerevisae*. Table 6 (in Supplementary information) illustrates some useful facts about our analysis on 14 metabolic pathways in *H. sapiens* using Method 1. Based on the average clustering coefficient (Table 8 in Supplementary information), the metabolic pathways designated by $HN_2$, $HN_3$–$HN_{14}$ are scale-free in nature (Table 8 in Supplementary information). In our study $HN_1$ does not follow power-law, thus having a random distribution. The average clustering coefficient of only 2 metabolic pathways $HN_2 = 0.10$ and $HN_{14} = 0.001$, whereas the rest of the networks have $avgC_i = 0$. Thus, none of the networks satisfy the criteria for $avgC_i$ and thus cannot be categorized under hierarchical group.

The breakdown points have been identified by performing an external perturbation and removing the metabolites using random and targeted means. A targeted approach incorporates a sense of bias for metabolite selection whereas a random approach removes the bias for selection.

We have also noticed a fact that even if a network follows power-law the exact breakdown point cannot be identified. They are $HN_{11}$ (random removal) and $HN_3$—$HN_{14}$ (targeted removal). On the other hand, networks where breakdown points can be identified include $HN_2$–$HN_9$, $HN_{12}$–$HN_{14}$ (random removal) and $HN_2$ (targeted removal). Furthermore, the breakdown points in $HN_2$ are N-acetyl-neuraminate 9P (connectivity = 2, random) and N-acetyl D-mannosamine (connectivity = 2, random) (Kimura et al., 2007). Similarly, the breakdown points in $HN_3$ are Crotonyl-CoA (connectivity = 3, random) with (*S*)-3-hydroxy-3-methylglutaryl-CoA as a 'core metabolite' in 'giant component' (Fig. 4c) (Higai et al., 2007). Now, we use Method 2 (Table 7 in Supplementary information). It successfully detects breakdown points in some metabolic networks not following a power law distribution, even though they could not be identified using Method 1. Metabolic networks whose breakdown points could be detected include $HN_2$–$HN_{10}$, $HN_{13}$–$HN_{14}$ (random removal) and $HN_2$–$HN_{10}$, $HN_{12}$–$HN_{14}$ (targeted removal). Furthermore, some useful insights can be highlighted in this regard. Method 1 revealed that the breakdown points in $HN_2$ are N-acetyl-neuraminate 9P (random), whereas using Method 2, N-acetyl α-D-glucosamine (connectivity = 3, random) has been identified as breakdown points. Also, N-acetyl α-D-glucosamine 6P has been identified as a 'core metabolite' in 'giant component'. Similarly in case of targeted removal, Method 2 detects D-glucosamine 6P

(connectivity = 2) and N-acetyl D-mannosamine (connectivity = 3) as breakdown metabolites. Furthermore, in case of $HN_3$, Method 2 reveals the breakdown points as acetoacetate (connectivity = 3, random) and (*S*)-3-hydroxy-3-methyl pregnenolone (connectivity = 2, random), and acetoacetyl-CoA (connectivity = 2, targeted) and (S)-3-hydroxy butanoyl-CoA (connectivity = 2, targeted).

Furthermore, in our study the core metabolite of giant component has been identified in $HN_2$ and $HN_3$ (Method 1). Using Method 1, we have found that in $HN_2$, have N-acetyl α-D-glucosamine 6P acts as a 'core metabolite' in 'giant component'. Similarly, in $HN_3$, (*S*)-3-hydroxy-3-methylglutaryl-CoA is the core metabolite having connectivity with acetyl-CoA, acetoacetate, acetoacetyl-CoA. Using Method 2, the core metabolite of the giant component is detected in $HN_2$–$HN_9$, $HN_{12}$–$HN_{14}$. The consistency of Methods 2 and 1 can be seen as the core metabolites for $HN_3$ detected by both the methods are the same. In some pathways, Method 2 has been able to detect the core metabolite of giant component but not Method 1. These are $HN_3$, $HN_5$, $HN_6$–$HN_9$ and $HN_{12}$–$HN_{14}$.

### 3.3. Analyzing breakdown points in merged carbohydrate metabolic network in S. cerevisae and H. sapiens

In the previous sections, we have used 12 metabolic pathways under carbohydrate metabolism in *S. cerevisae* and studied them separately. Now we combine the metabolic pathways for checking their combined effect of metabolite removal on the complete carbohydrate metabolism (Table 9 in Supplementary information). As the breakdown metabolites found under each category are large in number, we identify the most significant ones. The strategy employed by us deals with identifying the common linked metabolites between metabolic pathways under each category. This is due to the fact that if the breakdown metabolite detected by the method happens to be one of the common linked metabolites, it would cause a major effect on the working of both the pathways. Also, the information flow between the metabolic pathways gets hampered. The common linked metabolites found in carbohydrate metabolism in *S. cerevisae* are GDP-mannose ($YN_1$–$YN_3$), UDP-glucose ($YN_1$–$YN_{12}$), D-glucose 1P ($YN_1$–$YN_{12}$), pyruvate ($YN_2$–$YN_{10}$), butanoyl-CoA ($YN_2$–$YN_{10}$), acetoacetate ($YN_2$–$YN_{10}$), β-D-fructose 6P ($YN_3$–$YN_6$, $YN_3$–$YN_7$, $YN_6$–$YN_7$), D-glyceraldehyde-3-P ($YN_6$–$YN_7$) and acetyl-CoA ($YN_{10}$–$YN_{11}$) (Table 10 in Supplementary information). As these metabolites also act as common linked metabolites, probability that they act as breakdown metabolites is high. The reason is that, removal of these common linked metabolites results in disconnecting an important link between two or more metabolic pathways, which may result in causing harm to both the connected pathways. Table 11 (in Supplementary information) gives information about the final breakdown metabolites in each metabolic pathway under carbohydrate metabolism in *S. cerevisae*.

After performing the breakdown analysis on 14 individual metabolic pathways under carbohydrate metabolism in *H. sapiens*, we have employed the same strategy on the complete metabolism as a whole. Table 12 (in Supplementary information) presents the result of our analysis on metabolic pathways under carbohydrate metabolism in *H. sapiens*. Similarly, Table 13 (in Supplementary information) lists the common linked metabolites under each category. Now we check whether any of the common linked metabolites are the breakdown metabolites identified using our strategy. These identified metabolites are highly susceptible to breakdown and their removal hampers the functioning of metabolic pathways on the global scale, as they act as a connecting link between two or more metabolic pathways (Takemoto and Oosawa, 2007).

Now, we analyze the effect of breakdown metabolites on local as well as global metabolic networks. Local network study deals with studying their role restricted to one metabolic pathway only. But, role of breakdown metabolites can be better understood if their effect is studied on a global scale, i.e., studying their role in the complete metabolic network, rather than restricting to a single pathway. For example, in case of aminosugars metabolism ($HN_2$) in *H. sapiens*, the breakdown metabolites identified are N-acetyl neuraminate-9P (random, Method 1), N-acetyl-D-mannosamine (targeted, Method 1), N-acetyl α-D-glucosamine (random, Method 2), D-glucosamine-6P (targeted, Method 2), N-acetyl-D-mannosamine (targeted, Method 2) respectively. Now, for studying the role of these breakdown metabolites on the global scale, we have merged the aminosugars metabolism with all other metabolic pathways under carbohydrate metabolism giving rise to 14 metabolic pathways under carbohydrate metabolism. For checking whether these metabolites have a role on the global scenario and effect on all the other 13 metabolic pathways, we identify whether they are present as a common link within the metabolic pathways (Tables 13 in Supplementary information). But, it is evident that they do not act as common linked metabolites in any of the other metabolic pathways, thus explaining the fact that they do not have a global impact on their removal, but restricted to aminosugars metabolism only. Similarly, in case of fructose mannose metabolism ($HN_4$) in *H. sapiens*, breakdown metabolites found are β-D-fructose-6P (random, Method 1), D-mannose-6P (random, Method 2), β-D-fructose-2P (targeted, Method 2), l-fucose-1P (targeted, Method 2), D-glyceraldehyde-3P (targeted, Method 2) respectively. Checking their role on the global scenario, we find that β-D-fructose-6P is existent in glycolysis and pentose phosphate pathway; D-mannose-6P and L-fructose-1P are present in nucleotide sugars metabolism; L-fucose-1P is present in nucleotide sugars metabolism; D-glyceraldehyde-3P exists in galactose metabolism, glycolysis, pentose phosphate pathway, inositol phosphate metabolism and pentose glucuronate inter-conversion respectively. Thus, removing any of these metabolites drastically effects other associated reactions present in other metabolic pathways (Table 14 in Supplementary information) (Cohen et al., 2000).

### 3.4. Studying the hierarchical nature of breakdown points in carbohydrate metabolism in S. cerevisae and H. sapiens

Fig. 5a and b shows the hierarchical representation of breakdown metabolites in carbohydrate metabolism in *S. cerevisae*. As far as KEGG database is concerned, the carbohydrate metabolism in *S. cerevisae* consists of 12 metabolic pathways, and we have studied the hierarchical knockout pattern in carbohydrate metabolism. We find two distinct knockout patterns (Steinbrck et al., 2010). The first one initiates with phosphoenolpyruvate whose knockout results in removal of acetaldehyde and oxaloacetate. Removing oxaloacetate results in knockout of malonyl coA, acetyl coA, pyruvate and glyoxylate. The removal of a single metabolite like phosphoenolpyruvate effects the functioning of 9 successive metabolites (Fig. 5a). The second hierarchical knockout pattern has initiated with β-D-fructose-6P, resulting in removal of 8 directly successive metabolites with overall affecting around 20 successive metabolites (Fig. 5b). Table 15 (in Supplementary information) gives information about the list of backup reactions for the breakdown metabolites that are responsible for generating a hierarchy of breakdown metabolites.

Fig. 5c and d shows the hierarchical representation of breakdown metabolites in carbohydrate metabolism in *H. sapiens*. As already discussed, β-D-fructose-6P, in case of fructose mannose metabolism in *H. sapiens*, acts as a breakdown point. We have started with this metabolite and tried to track the effect

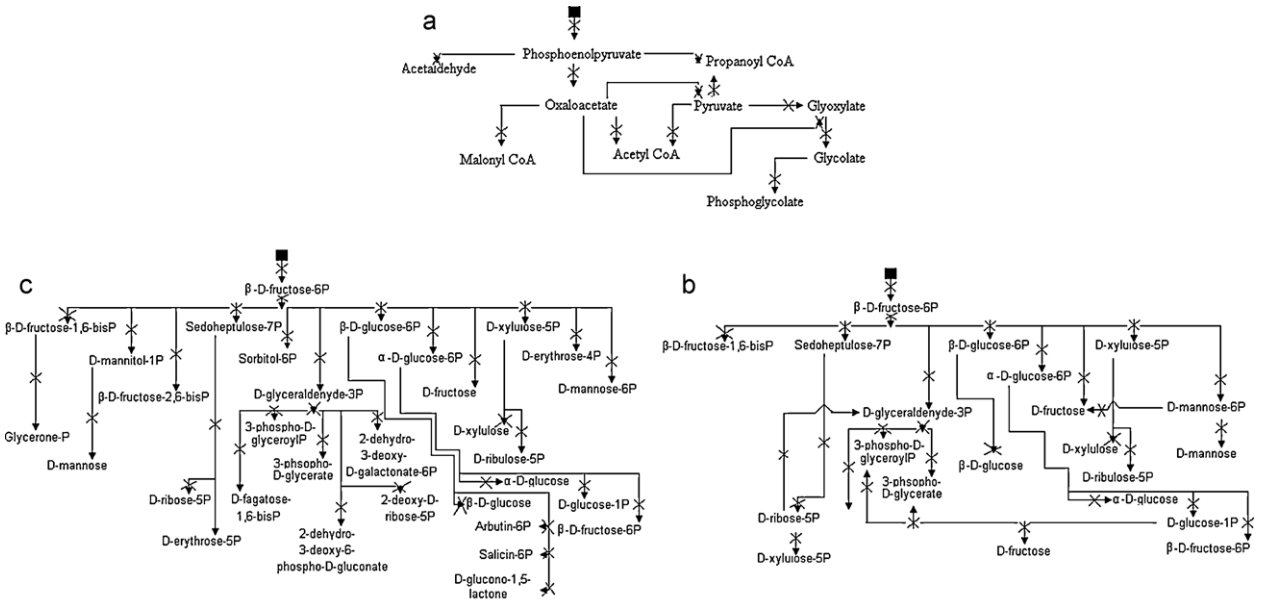


**Fig. 5.** Breakdown hierarchy: (a) *S. cerevisae* (knockout pattern 1), (b) *S. cerevisae* (knockout pattern 2), (c) *H. sapiens*.

of this metabolite removal on the other metabolites. KEGG database contains information on 14 metabolic pathways under carbohydrate metabolism in *H. sapiens*. Since β-D-fructose-6P appears many times in the entire metabolic network under carbohydrate metabolism in *H. sapiens*, we have checked the effect of removing β-D-fructose-6P, which leads to the knock-out of several other metabolites. We propose that corresponding metabolite removal is hierarchical in nature, i.e., the knock-out of one metabolite is dependent on its predecessor knocked-out metabolite. For instance, β-D-fructose-6P acts as a breakdown metabolite in metabolic pathways '$HN_4$', '$HN_6$' and '$HN_7$'. Removing this metabolite effects the functioning of other metabolites that act as its successor. For example, β-D-fructose-6P participates in 12 reactions in carbohydrate metabolism, and all these reactions get effected with its removal, leading to the knockout of 12 primary metabolites like β-D-fructose-1,6-bisP; D-mannitol-1P; β-D-fructose-2,6-bisP; sedoheptulose-7P; sorbitol-6P; D-glyceraldehyde-3P; β-D-glucose-6P; α-D-glucose-6P; D-fructose; D-xylulose-5P; D-erythrose-4P and D-mannose-6P. This leads to the knockout of several other successive metabolites present in other metabolic pathways. But, another important fact that we should keep in mind is that all the metabolic pathways are inter-linked and there are always certain back-up reactions to produce these metabolites, even if we block any one of the reactions. For example, D-glyceraldehyde-3P is also produced from 6 different reactions present in the metabolic pathways '$HN_4$', '$HN_5$', '$HN_6$', '$HN_7$', '$HN_9$'. Similarly, other knocked-out metabolites like α-D-glucose-6P in '$HN_5$', '$HN_6$', '$HN_7$', '$HN_{14}$', D-fructose in '$HN_4$', '$HN_5$', '$HN_{14}$', D-xylulose-5P in '$HN_1$', '$HN_{10}$', '$HN_{11}$', D-mannose-6P in '$HN_4$', '$HN_{10}$' too have back-up reactions (Table 16 in Supplementary information) (Higai et al., 2007).

### 3.5. Calculating resilience and fitness measures for carbohydrate metabolism in S. cerevisae

We have tested our algorithm (Methods 1 and 2) on 12 metabolic pathways of *S. cerevisae*, and calculated their targeted (TR) as well as random resilience (RR) measures. Tables 17 and 18 (in Supplementary information) present all the values that are obtained after this calculation using Methods 1 and 2 respectively. Using Method 1 (Table 17 in Supplementary information), metabolic pathways for which resilience due to targeted node cannot be calculated are $YN_2$–$YN_{11}$. The targeted resilience measure varies from 1.65 to 10.2%. Network $YN_1$ has the highest targeted resilience of 10.2%. Similarly, $YN_{12}$ has the lowest resilience of 1.65% (Agrawal and Whitlock, 2011). The random resilience measure ranges in 22.87–43.07%. Network $YN_{10}$ has the highest targeted resilience of 43.07%. Similarly, $YN_9$ has the lowest resilience of 22.87%. In case of Method 2 (Table 18 in Supplementary information), the targeted resilience score varies from 1.2 to 11.2% as compared to 1.65–10.2% (Method 1). Method 2 predicts that $YN_1$ has the highest targeted resilience score of 3.4–11.2%. Similarly, one of the lowest targeted resilience score is seen for $YN_4$ in 1.2–1.9%. The random resilience score varies in 21.45–53.34%. Network $YN_2$ has the highest random resilience score of 37.12–53.34%, whereas the lowest resilience score of 21.45–23.65% is found in $YN_9$.

We have already defined 'fitness' of a metabolite as its degree of resistance against knock-out. We have defined some basic categories of fitness, namely, *strong fitness*, *weak fitness* and *neutral fitness*. A metabolite has strong fitness if its breakdown does not result in breakdown of the entire metabolic pathway, due to its production by backup reactions. As discussed in the previous sections, we also find 'fitness' of breakdown metabolites in *S. cerevisae* (Table 19 in Supplementary information). For example, GDP-mannose has a strong fitness effect due to 8 backup reactions. A weak fitness effect of a metabolite is existent if it does not have any alternate reaction for production in case of metabolite removal. Butanoyl-CoA has a weak fitness effect due to only 1 backup reaction. Finally, neutral fitness happens when the knockdown of a metabolite occurs after the breakdown of the metabolic pathway has already occurred. None of the metabolites show weak fitness effect. We have also studied the relation between fitness and resilience score of metabolic pathways in carbohydrate metabolism in *S. cerevisae* (Fig. 6a). It shows that with increase in fitness, the resilience score also increases. The reason being, with fitness of a metabolite is related to its presence in the number of alternate reactions in the metabolic pathway, which results in greater resilience value too.

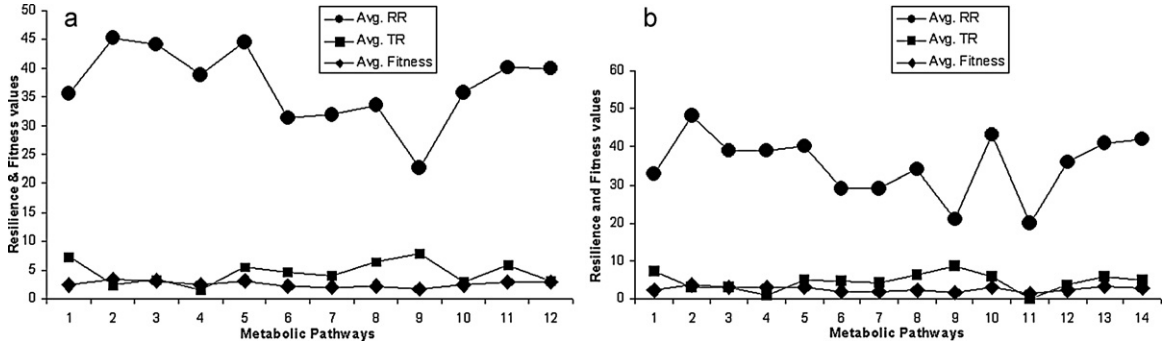


**Fig. 6.** Distribution of resilience and fitness: (a) *S. cerevisae*, (b) *H. sapiens*.

### 3.6. Calculating resilience and fitness measures for carbohydrate metabolism in H. sapiens

Tables 20 and 21 (in Supplementary information) present all the values that are obtained after resilience calculation using Methods 1 and 2 respectively. First we consider Method 1 (Table 20 in Supplementary information). In this case, '0' represents those values whose measures cannot be calculated. This situation arises for the networks $HN_1$, $HN_3$, $HN_4$, $HN_5$, $HN_6$–$HN_9$, $HN_{10}$, $HN_{12}$, $HN_{13}$ whose resilience due to targeted node removal cannot be calculated. Similarly, for network $HN_1$ random resilience cannot be calculated. In case of $HN_2$ and $HN_{14}$ the targeted as well as random resilience scores are found to be 9.3%, 32.55% and 2.08%, 37.5% respectively. One of the highest targeted resilience score is found for $HN_6$, which is around 9.3% (Westerhoff et al., 2009).

In case of Method 2 (Table 21 in Supplementary information), networks for which resilience score cannot be calculated are $HN_1$ and $HN_{11}$ due to targeted removal, whereas $HN_1$ due to random metabolite removal. The targeted resilience measure varies in 0–10%. Network $HN_6$ (glycolysis) has the highest targeted resilience of 10%, because breakdown occurs after removing one node specifically from out of 13. Similarly, $HN_{10}$ (glyoxylate and dicarboxylate metabolism) has the lowest resilience of 0%. The random resilience measure ranges in 20–56%. Network $HN_3$ (butanoate metabolism) has the highest targeted resilience of 56%, because breakdown occurs after removing 11 specific nodes from out of 20. Similarly, $HN_8$ (aminosugar metabolism) and $HN_{10}$ (glyoxylate and dicarboxylate metabolism) have the lowest resilience of 20%, as they require 17 nodes to be removed out of 87 nodes and 10 nodes to be removed out of 50 nodes for breakdown of the network.

The targeted resilience score varies in 0–9.3% as compared to 1.35–9.3% (Method 1). Method 2 predicts that $HN_2$ has the highest targeted resilience score of 10% that correlates the value as predicted by Method 1 too. Similarly, some of the lowest targeted resilience score is seen for $HN_3$ (butanoate metabolism) as 2.5–3.7%, for $HN_4$ (fructose mannose metabolism) as 2.1–4.2%, for $HN_5$ (galactose metabolism) as 0.5–1.3% and for $HN_{14}$ (starch and sucrose metabolism) as 2.5–4.7%. Furthermore, the random resilience score varies in 0–56% as compared to 0–42.85% (Method 1). Network $HN_3$ (butanoate metabolism) has the highest random resilience score of 40–56%. Similarly, some of the lowest random resilience scores are seen for networks $HN_1$ (glycolysis) as 0%, $HN_9$ (inositol phosphate metabolism) as 20–22%. We have observed that the pathways are more resilient to random attacks than targeted attack as the breakdown occurs after more nodes removed randomly than targeted.

We have also found the fitness of individual metabolites in metabolic pathways under carbohydrate metabolites in *H. sapiens*. For instance, α-D-glucose-6P acting as a breakdown metabolite in aminosugars metabolism is produced as it appears in back-up 19 reactions in carbohydrate metabolism resulting in strong fitness (Table 22 in Supplementary information). Similarly, D-mannitol-1P acting as a breakdown metabolite in fructose and mannose metabolism does not have any back-up reaction for its production thus causing a permanent effect on the metabolic pathway, and showing weak fitness effect. Lastly, breakdown in aminosugars metabolism occurs after N-acetyl-α-D-glucosamine-6P is knocked-out (Method 1, targeted attack). We have tried removing N-acetyl-D-mannosamine-6P again (Method 1, targeted attack) resulting in no effect, as the metabolic pathway already broke down. This kind of effect is termed as neutral fitness (Higai et al., 2007). Furthermore, Fig. 6b shows the relation between fitness and resilience score in metabolic pathways under carbohydrate metabolism in *H. sapiens*. This also coincides with our results in *S. cerevisae* (Fig. 6a) where with increase in fitness resilience increases.

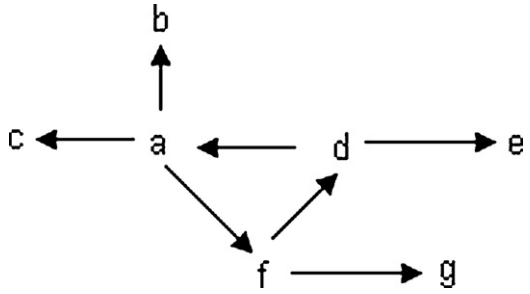


**Fig. 7.** Schematic sketch of metabolic pathway.

Similarly, the breakdown probability of each metabolite in a metabolic network differs on the basis of the strategy chosen, i.e., random attack or targeted attack. The breakdown probability of each metabolite is calculated on the basis of its number of incoming and outgoing links. In Fig. 7, breakdown probabilities (targeted), *tbp*, are calculated on the basis of number of incoming links to the total number of links for a metabolite whereas, breakdown probabilities (random), *rbp*, are calculated on the basis of the random chance of selection of a metabolite. Thus, $tbp(a) = 1/4$, $tbp(b) = 1$, $tbp(c) = 1$, $tbp(d) = 1/3$, $tbp(e) = 1$, $tbp(f) = 1/3$, $tbp(g) = 1$ and breakdown probabilities (random) are $rbp(a) = 1/7$, $rbp(b) = 1/7$, $rbp(c) = 1/7$, $rbp(d) = 1/7$, $rbp(e) = 1/7$, $rbp(f) = 1/7$, $rbp(g) = 1/7$. The targeted as well as random breakdown probability of metabolites in aminosugars metabolism in *H. sapiens* is given in Table 23 (in Supplementary information).

## 4. Conclusions

We have used power-law modeling and graph-theoretical approaches for analyzing the extent of robustness of 12 metabolic pathways under carbohydrate metabolism in *S. cerevisae* and 14 metabolic pathways under carbohydrate metabolism in *H. sapiens*. We have also performed simulation of various mutational events by performing some external perturbations. The metabolites which

are absolutely essential for the overall functioning of the pathway and whose removal causes a breakdown in power-law plot are termed as 'breakdown metabolites'. We have performed both random as well as targeted removal of metabolites. The power-law modeling helps in detecting the exact 'breakdown point' after random and targeted metabolite removal. Our algorithm successfully identifies these metabolites too. We have also identified 'core metabolite' of 'giant component'. The giant component is highly connected metabolites and are presumed to be very old in network life cycle as compared to other metabolites that originate from these metabolites. The 'core metabolite' has the highest connected neighbors. Our algorithm has two methods that differ in the manner in which metabolites are removed from the metabolic network. Method 1 does not add the removed metabolite back into the network, whereas Method 2 adds the removed metabolite back into the network. Method 1 identifies the combined effect of many removed metabolites on the network, whereas using Method 1 the individual metabolite contributions can be identified.

We have showed that with increase in fitness of a metabolite, the resilience of the entire metabolic pathway increases. This is due to the fact that the number of reactions by which a single metabolite is formed can be more than one. That is, fitness of the metabolite is high as well as the resilience value of the metabolic pathway involving the metabolite. An exception can also occur in this case, where the overall resilience of a metabolic pathway can be less, though some of the breakdown metabolites have good fitness score. A metabolite has strong fitness if the knockout of one of its preceding metabolite does not result in breakdown of the entire metabolic pathway, due to its production through other reactions. A weak fitness effect of a metabolite is existent if it does not have any alternate reaction for its production in case of removal of its preceding metabolite. A neutral fitness happens when the knockdown of a metabolite occurs after the breakdown of the metabolic pathway has already occurred. Furthermore, 'targeted breakdown probability', i.e., the ratio of number of incoming links to a metabolite to the total number of incoming and outgoing links for the metabolite is always higher than 'random breakdown probability', i.e., the random chance of selecting a metabolite from the metabolic network that can act as a breakdown metabolite.

Similarly, 'random resilience scores', i.e., ratio of number of metabolites removed randomly until power law breaks to the total number of metabolites, for a metabolic network is always higher than that of 'targeted resilience scores', i.e., ratio of number of metabolites removed in targeted manner until power law breaks to the total number of metabolites. Also, in case of *S. cerevisae*, breakdown has occurred after 35.09–39.03% of metabolites have been knocked-out using random attack and after 3.39–5.43% of metabolites have been knocked-out using targeted attack. In *H. sapiens*, breakdown has occured after 33.57–36.35% of metabolites have been knocked-out using random attack and after 3.53–5.3% of metabolites have been knocked-out using targeted attack. The external perturbation performed by us emphasizes on the fact that common random mutational events can give rise to a change in metabolic networks. A mutational event in a metabolite can seriously disturb its activity to for the next product and ultimately hampers the corresponding reaction. We have also found that metabolic networks with power-law degree distribution fragments less easily into large disconnected sub-networks upon random node removal whereas they are more susceptible to targeted attacks. Also, resilience is high against random node removal but low against targeted node removal.

## Appendix A. Supplementary data

Supplementary data associated with this article can be found, in the online version, at doi:10.1016/j.compbiolchem.2011.10.007.

## References


Acencio, M.L., Lemke, N., 2009. Towards the prediction of essential genes by integration of network topology, cellular localization and biological process information. BMC Bioinformatics 10, 290.

Adami, C., Hintze, A., 2008. Evolution of complex modular biological networks. PLoS Comput. Biol. 4 (Suppl. 5), e23.

Agrawal, A.F., Whitlock, M.C., 2011. Inferences about the distribution of dominance drawn from yeast gene knockout data. Genetics 187 (Suppl. 2), 553–566.

Arita, M., 2005. Scale-freeness and biological networks. J. Biochem. 138 (Suppl. 1), 1–4.

Barabasi, A.L., Albert, R., 2002. Statistical mechanics of complex networks. Rev. Mod. Phys. 74, 47–97.

Barabasi, A.L., Albert, R., Jeong, H., 2000. Error and attack tolerance of complex networks. Nature 406, 378–382.

Bongard, J., Lipson, H., 2007. Automated reverse engineering of nonlinear dynamical systems. Proc. Natl. Acad. Sci. U.S.A. 104 (Suppl. 24), 9943–9948.

Bulik, S., Grimbs, S., Huthmacher, C., Selbig, J., Holzhtter, H.G., 2009. Kinetic hybrid models composed of mechanistic and simplified enzymatic rate laws – a promising method for speeding up the kinetic modelling of complex metabolic networks. FEBS J. 276 (Suppl. 2), 410–424.

Bullmore, E., Sporns, O., 2009. Complex brain networks: graph theoretical analysis of structural and functional systems. Nature 10, 186–198.

Callaway, D.S., Newman, M.E., Strogatz, S.H., Watts, D.J., 2000. Network robustness and fragility: percolation on random graphs. Phys. Rev. Lett. 85 (Suppl. 25), 5468–5471.

Cohen, R., Erez, K., ben-Avraham, D., Havlin, S., 2000. Resilience of the internet to random breakdowns. Phys. Rev. Lett. 85 (Suppl. 21), 4626–4628.

Destexhe, A., Touboul, J., 2010. Can power-law scaling and neuronal avalanches arise from stochastic dynamics? PLOS One 5 (Suppl. 2), e8982.

Deo, N., 2003. Graph Theory: With Applications To Engineering And Computer Science. Prentice Hall India.

Doyle III, G.J., Stelling, J., 2009. Systems interface biology. J. R. Soc. Interface 3, 603–616.

Glass, L., Siegelmann, H.T., 2000. Logical and symbolic analysis of robust biological systems. Curr. Opin. Genet. Dev. 20 (Suppl. 6), 644–649.

Hacking, D.F., 2008. 'Knock, and it shall be opened': knocking out and knocking in to reveal mechanisms of disease and novel therapies. Early Hum. Dev. 84 (Suppl. 12), 821–827.

Higai, K., Miyazaki, N., Azuma, Y., Matsumoto, K., 2007. Interleukin-1beta induces sialyl Lewis X on hepatocellular carcinoma HuH-7 cells via enhanced expression of ST3Gal IV and FUT VI gene. FEBS Lett. 580 (Suppl. 26), 6069–6075.

Jeong, H., Tombor, B., Albert, R., Oltvai, Z.N., Barabaasi, A.L., 2000. The large-scale organization of metabolic networks. PNAS 407 (Suppl. 5), 651–654.

Kawashima, S., Okuno, Y., Hattori, M., Kanehisa, M., Goto, S, 2004. The Kegg resource for deciphering the genome. Nucleic Acids Res. 32, D277–D280.

Kimura, N., Ohmori, K., Miyazaki, K., Izawa, M., Matsuzaki, Y., Yasuda, Y., Takematsu, H., Kozutsumi, Y., Moriyama, A., Kannagi, R., 2007. Human B-lymphocytes express alpha2-6-sialylated 6-sulfo-N-acetyllactosamine serving as a preferred ligand for CD22/Siglec-2. J. Biol. Chem. 282 (Suppl. 44), 32200–32207.

Kitano, H., 2007. Towards a theory of biological robustness. Mol. Syst. Biol. 3, 137.

Kitano, H., 2001. Foundations of Systems Biology. MIT Press, Cambridge.

Kreeger, P.K., Lauffenburger, D.A., 2010. Cancer systems biology: a network modeling perspective. Carcinogenesis 31 (Suppl. 1), 2–8.

Macia, J., Sol, R.V., 2009. Distributed robustness in cellular networks: insights from synthetic evolved circuits. J. R. Soc. Interface 6 (Suppl. 33), 393–400.

Mendes, P., Messiha, H., Malys, N., Hoops, S., 2009. Enzyme kinetics and computational modeling for systems biology. Methods Enzymol. 467, 583–599.

Minnhagen, P., Bernhardsson, S., 2008. The blind watchmaker network: scale-freeness and evolution. PLoS One 3 (Suppl. 2), e1690.

Mitzenmacher, M., 2003. A brief history of generative models for power law and lognormal distributions. Internet Math. 1, 226–251.

Palsson, B., 2006. Systems Biology: Properties of Reconstructed Networks. Cambridge Univ. Press, Cambridge.

Ravasz, E., 2009. Detecting hierarchical modularity in biological networks. Methods Mol. Biol. 541, 145–160.

Rikvold, P.A., 2007. Self-optimization, community stability, and fluctuations in two individual-based models of biological coevolution. J. Math. Biol. 55 (Suppl. 5–6), 653–677.

Schmidt, H., Jacobsen, E.W., 2004. Linear systems approach to analysis of complex dynamic behaviours in biochemical networks. Syst. Biol. (Stevenage). 1 (Suppl. 1), 149–158.

Schmidt, S., Rainieri, S., Witte, S., Matern, U., Martens, S., 2011. Identification of a *Saccharomyces cerevisae* glucosidase that hydrolyzes flavonoid glucosides. Appl. Environ. Microbiol. 77 (Suppl. 5), 1751–1757.

Steinbrck, L., Pereira, G., Efferth, T., 2010. Effects of artesunate on cytokinesis and G2/M cell cycle progression of tumour cells and budding yeast. Cancer Genomics Proteomics 7 (Suppl. 6), 337–346.

Stumpf, M.P.H., de Silva, E., 2005. Complex networks and simple models in biology. J. R. Soc. Interface 2, 419–430.

Sudakov, B., Vu, V.H., 2008. Local Resilience of Graphs, vol. 33. Wiley InterScience, pp. 409–433.

Takemoto, K., Oosawa, C., 2007. Modeling for evolving biological networks with scale-free connectivity, hierarchical modularity, and disassortativity. Math. Biosci. 208 (Suppl. 2), 454–468.

Westerhoff, H.V., Kolodkin, A., Conradie, R., Wilkinson, S.J., Bruggeman, F.J., Krab, K., van Schuppen, J.H., Hardin, H., Bakker, B.M., Mon, M.J., Rybakova, K.N., Eijken, M., van Leeuwen, H.J., Snoep, J.L., 2009. Systems biology towards life in silico: mathematics of the control of living cells. J. Math. Biol. 58 (Suppl. 1–2), 7–34.
Wit, E., Khanin, R., 2006. How scale-free are biological networks. J. Comput. Biol. 13 (Suppl. 3), 810–818.
Zeng, A., Ma, H., 2003. The connectivity structure, giant strong component and centrality of metabolic networks. Bioinformatics 19 (Suppl. 11), 1423–1430.
Zhang, J., Zhang, Z., 2009. A big world inside small-world networks. PLOS One 4 (Suppl. 5), e5686.